Sustainable Thermoplastic Elastomers Produced *via* Cationic RAFT Polymerization

*Scott W. Spring, Red O. Smith-Sweetser, Stephanie I. Rosenbloom, Renee J. Sifri, and Brett P. Fors**

Department of Chemistry and Chemical Biology, Cornell University, Ithaca, New York 14853, United States

Supporting Information

Experimental Section

Materials

Isobutyl vinyl ether (IBVE) (99%, TCI), 1,4-butanediol divinyl ether (98%, Millipore Sigma), *p*-methoxystyrene (MOS) (from synthesis or purchased; 98%, TCI) and 2,3-dihydrofuran (DHF) (99%, TCI) were dried over calcium hydride (CaH_2) (ACROS organics, 93% extra pure, 0–2 mm grain size) for 12 hours, distilled under vacuum, and degassed by three freeze-pump-thaw cycles. Ferrocenium tetrafluoroborate ($FcBF_4$) (97%, Millipore Sigma), HCl in Et_2O (2.0 M, Millipore Sigma), *p*-coumaric acid (98%, TCI), butylated hydroxytoluene (BHT) (99%, Millipore Sigma), triethylamine (anhydrous, 99.5%, Millipore Sigma), potassium carbonate (anhydrous, 99%, Millipore Sigma), and methyl iodide (98%, Alfa Aesar) were used as received. Sodium N,N-diethyldithiocarbamate trihydrate (98%, Alfa Aesar) was azeotropically dried with benzene. Dichloromethane (DCM), diethylether (Et_2O), and toluene were purchased from J.T. Baker and were purified by purging with argon for 1 hour, followed by passing through two packed columns of neutral alumina under argon pressure. Hexanes and ethyl acetate were purchased from Fischer scientific and used as received.

General Measurements

All polymer samples were analyzed using a Tosoh EcoSec HLC 8320 GPC system with two SuperHM-M columns in series at a flow rate of 0.350 mL/min. THF was used as the eluent and number-average molecular weights (M_n), weight-average molecular weights (M_w), and dispersities ($Đ$) for PIBVE were determined by light scattering using a Wyatt miniDawn

Treos multi-angle light scattering detector and a calculated dn/dc value of 0.0381 mL g^{-1}. The reported M_ns for triblock copolymers were calculated from refractive index chromatograms against TSKgel polystyrene standards. Nuclear magnetic resonance (NMR) spectra were recorded on a Varian 400 MHz, a Varian 600 MHz, or a Bruker 500 MHz instrument.

Synthesis of *p*-methoxystyrene

p-Coumaric acid (25g, 0.15 mol) and BHT (150 mg, 0.5 wt%) were added to an oven dried flask equipped with a reflux condenser and were dissolved in 70 mL of DMF under nitrogen. Triethylamine (43 mL, 0.31 mol) was added and the reaction mixture was heated to 100 °C and stirred for 6 hours. Triethylamine was then removed *via* rotary evaporation and K_2CO_3 (21g, 0.15 mol) was added, followed by addition of methyl iodide (12.2 mL, 0.20 mol). The reaction mixture was heated to 40 °C and stirred overnight. The reaction was quenched with NaOH (15 mL, 3M) and diluted with H_2O (80 mL). The organic layer was separated, and the aqueous layer extracted with ethyl acetate (3 x 20 mL). The combined organic layers were then washed with H_2O (10 x 20mL), followed by brine, then dried over $MgSO_4$ before being filtered and concentrated in vacuo to yield a dark brown liquid. Fractional distillation at 60 °C under ~300 mtorr vacuum gave a 44 °C vapor that condensed to yield 15.7g (77% yield) of clear, colorless *p*-methoxystyrene. This was dried over CaH_2 and distilled again before use. ^{1}H and ^{13}C NMR were consistent with previous literature reports.[1]

^{1}H NMR (500 MHz, $CDCl_3$, δ, ppm): 7.36 (m, 2H), 6.87 (m,2H), 6.68 (dd, J = 17.6, 10.9 Hz, 1H), 5.62 (d, J = 17.6 Hz, 1H), 5.14 (d, J = 10.7 Hz, 1H), 3.82 (s, 3H). ^{13}C NMR (126 MHz, $CDCl_3$, δ, ppm) 159.52, 136.37, 130.59, 127.52, 114.05, 111.71, 55.43.

Synthesis of difunctional CTA

1,4-butanediol divinyl ether (0.64 mL, 4 mmol) was added dropwise to a flame-dried flask containing a stirring solution of HCl in diethyl ether (4.4 mL, 8.8 mmol) cooled to −78 °C under nitrogen. This solution was warmed to 0 °C and stirred for 2 hours to produce the chloroether adduct of the oxocabenium ion. In a separate flame-dried flask, sodium *N,N*-diethyl dithiocarbamate (2.1 g, 12 mmol) was dissolved in Et_2O (11 mL) and cooled to 0 °C under nitrogen. The chloroether solution was then added dropwise to the *N,N*-diethyl dithiocarbamate solution over 10 min. The reaction mixture was stirred at 0 °C for 2 hours before being warmed to room temperature and stirred an additional 3 hours. The reaction mixture was then diluted with sat. sodium bicarbonate and extracted with Et_2O (3 x 10 mL). The combined organic layers were then washed with brine and dried over $MgSO_4$ before being filtered and concentrated *via* rotary evaporation. The crude product was a dark red to yellow viscus oil. The product was purified by column chromatography using SiO_2 treated with 3% NEt_3 in hexanes. The column of treated SiO_2 was washed with 200 mL of the mobile phase (14% EtOAc in hexanes) before loading the crude oil. 666 mg (38% yield) of the pale-yellow product was isolated (r.f. = 0.33 in 14% EtOAc in hexanes).

^{1}H NMR (500 MHz, $CDCl_3$, δ, ppm): 5.90 (q, *J* = 6.3 Hz, 2H), 4.02 (q, *J* = 7.1 Hz, 4H), 3.82 – 3.67 (m, 6H), 3.62 – 3.52 (m, 2H), 1.72 (d, *J* = 6.2 Hz, 6H), 1.63 (hept, *J* = 2.5 Hz, 4H), 1.28 (dt, *J* = 9.4, 7.1 Hz, 12H). ^{13}C NMR (125 MHz, $CDCl_3$, δ, ppm): 195.00, 91.38, 91.36, 69.11, 69.06, 48.98, 46.99, 29.97, 26.33, 26.30, 23.61, 12.74, 11.79. ESI-MS (DART): [C18H36N2O2S4+Na^+] calc.: 463.15518, obs.: 463.15491.

Polymerization of PMOS-PIBVE-PMOS

All polymerizations were set up in a nitrogen glovebox. A solution of difunctional CTA in DCM (0.60 mL, 22 mg/mL, 0.03 mmol) and IBVE (2.60 mL, 20 mmol) were added to a 20 mL scintillation vial containing a stir bar. The polymerization was initiated by addition of $FcBF_4$ in DCM (1.1 mL, 1 mg/mL, 0.02 mol% relative to CTA) and the reaction mixture was stirred until IBVE reached >95% conversion by NMR, typically 6 hours. The solution was then diluted with DCM before adding *p*-methoxystyrene and additional $FcBF_4$ (1.1 mL, 1mg/mL, 0.02 mol% relative to CTA) to achieve a total volume of 9 mL. This mixture was then stirred for 20 hours, or until *p*-methoxystyrene conversion reached ~60% conversion. The polymerization was then terminated with sodium *N,N*-diethyl dithiocarbamate (2 equiv relative to CTA) and diluted with DCM. The polymer was precipitated in 1.5 L of stirring MeOH twice before vacuum drying at 80 °C for 48 hours. f_{HB} was calculated from integration of peaks 6.89 – 6.18 and 0.90 ppm in accordance with Equation S1 and S2. ^{1}H NMR (500 MHz, $CDCl_3$, δ, ppm): 6.89 – 6.18 (m, 4H PMOS), 3.84 – 3.66 (m, 3H PMOS), 3.66 – 3.33 (m, 1H PIBVE), 3.33 – 3.03 (m, 2H PIBVE), 2.06 – 1.10 (m, 2H PIBVE, 3H PMOS), 0.90 (m, 6H PIBVE).

Equation S1:

$$x_{PMOS} = \frac{\frac{1}{4} i(6.89 - 6.18\, ppm, PMOS)}{\frac{1}{4} i(6.89 - 6.18\, ppm, PMOS) + \frac{1}{6} i(0.90\, ppm, PIBVE)}$$

Equation S2:

$$f_{HB} = \frac{x_{PMOS} \frac{mw_{MOS}}{\rho_{PMOS}}}{\left[x_{PMOS} \frac{mw_{MOS}}{\rho_{PMOS}} + (1 - x_{PMOS}) \frac{mw_{IBVE}}{\rho_{PIBVE}}\right]}$$

Where x_{PMOS} is the mole fraction of PMOS, mw_{MOS} is the molecular weight of MOS (134.18 g/mol), ρ_{PMOS} is the density of PMOS (0.962 g/mL), mw_{IBVE} is the molecular weight of IBVE (100.16 g/mol), and ρ_{PIBVE} is the density of PIBVE (0.920 g/mL).

Polymerization of PDHF-PIBVE-PDHF

All polymerizations were set up in a nitrogen glovebox. A solution of difunctional CTA in DCM (0.60 mL, 22 mg/mL, 0.03 mmol) and IBVE (2.60 mL, 20 mmol) were added to a 20 mL scintillation vial containing a stir bar. The polymerization was initiated by addition of $FcBF_4$ in DCM (1.1 mL, 1 mg/mL, 0.02 mol% relative to CTA) and the reaction mixture was stirred until IBVE reached >95% conversion by NMR, typically 6 hours. The solution was then diluted with DCM before adding DHF and additional $FcBF_4$ (1.1 mL, 1mg/mL, 0.02 mol% relative to CTA) to achieve a total volume of 8 mL. This was then stirred for an additional 20 hours, or until full conversion of DHF was reached. The polymerization was then terminated with sodium *N,N*-diethyl dithiocarbamate (2 equiv relative to CTA) and diluted with DCM. The polymer was precipitated in MeOH twice before vacuum drying at 80 °C for 48 hours. f_{HB} was calculated from integration of peaks 4.21 – 2.93 and 0.90 ppm in accordance with Equation S3 and S4. ^{1}H NMR (500 MHz, $CDCl_3$, δ, ppm): 4.21 – 2.93 (m, 3H PDHF, 3H PIBVE), 2.49 – 1.30 (m, 3H PDHF, 3H PIBVE), 0.90 (m, 6H PIBVE).

Equation S3:

$$x_{PDHF} = \frac{i(4.21 - 2.93\ ppm, PIBVE\ and\ PDHF) - \frac{1}{2}i(0.90\ ppm, PIBVE)}{i(4.21 - 2.93\ ppm, PIBVE\ and\ PDHF)}$$

Equation S4:

$$\mathrm{f}_{HB} = \frac{x_{PDHF}\frac{mw_{DHF}}{\rho_{PDHF}}}{\left[x_{PDHF}\frac{mw_{DHF}}{\rho_{PDHF}} + (1 - x_{PDHF})\frac{mw_{IBVE}}{\rho_{PIBVE}}\right]}$$

Where x_{PMOS} is the mole fraction of PDHF, mw_{DHF} is the molecular weight of DHF (70.09 g/mol), ρ_{PDHF} is the density of PDHF (1.04 g/mL), mw_{IBVE} is the molecular weight of IBVE (100.16 g/mol), and ρ_{PIBVE} is the density of PIBVE (0.920 g/mL).

Material Characterization

Triblock copolymers were pressed into dog-bone-shaped tensile bars using a 4120 Hydraulic Unit Carver heated press. The polymer samples were placed in the mold between two sheets of PTFE protective lining. PMOS-PIBVE-PMOS samples were pressed at 120 °C and 3,000 psi for 1 min. PDHF-PIBVE-PDHF samples were pressed at 160 °C and 3,000 psi for 1 min. The press was water cooled to room temperature before releasing pressure. Excess material was trimmed away with scissors to obtain dog-bone-shaped tensile bars with approximate gauge dimensions of 16 x 2.5 x 0.7 mm.

Tensile properties of the prepared samples were examined using a Zwick/Roell Z010 testing system equipped with pneumatic grips. Samples were stretched to break at an extension rate of 75 mm min^{-1}. Values reported are an average calculated from three samples. To study the hysteresis behavior of select elastic polymers, a cyclic loading of 300% strain at 50 mm min^{-1} was applied for 10 cycles.

For determination of thermal transitions, differential scanning calorimetry (DSC) was performed using a TA Instruments Q1000. Samples were placed in aluminum crucibles and heated to 200 °C at 20 °C min^{-1} to erase thermal history, cooled to −70 °C and held at this temperature for 10 min to equilibrate. A second heat cycle was performed to 200 °C at 20 °C min^{-1} during which the thermal data was collected. Thermogravimetric analysis (TGA) was performed using a TA Instruments Q500 where samples were heated at a rate of 20 °C min^{-1} from 25 °C to 500 °C.

Rheological tests were performed on a TA Instruments DHR3 rheometer using an 8mm parallel plate in a temperature controlled environmental test chamber under a nitrogen atmosphere. The sample was loaded onto the bottom parallel plate at 170°C and the top plate was lowered to a trim gap of 1050μm. Excess polymer material was trimmed and then the plate was

lowered to a gap of 1000μm. Strain sweeps (0.1–100%) at 170°C were first performed at 6.3 rad/s (1 Hz) to determine the linear viscoelastic region. A 1% strain was selected as it consistently lied within the linear viscoelastic region for the preceding range of frequencies. Before each frequency sweep, the sample was equilibrated at 170 °C for 5 min to ensure uniform sample temperature.

All small-angle X-ray scattering (SAXS) experiments were carried out at the Functional Materials Beamline (FMB) at the Cornell High Energy Synchrotron Source (CHESS). To prepare samples for SAXS, polymers were pressed into the center of stainless-steel washers (4.42 mm I.D., 9.53 mm O.D., 0.79 mm thickness) using a heated press. PMOS-PIBVE-PMOS samples were pressed under 3,000 psi of pressure at 120 °C for 1 min and PDHF-PIBVE-PDHF samples were pressed under 3,000 psi of pressure at 160 °C for 1 min. The washers were sealed between Kapton tape and annealed under vacuum at 140 °C for 48 h, followed by cooling to room temperature under vacuum. The Kapton tape-sealed washers containing the annealed samples were mounted directly onto the sample stage at CHESS for SAXS data acquisition. The X-ray energy of 15.89 keV was selected using a diamond (220) side bounce monochromator[2], and the beam size (0.3 x 0.3 mm^2, ca. 1 m upstream from the sample) was set using slits. SAXS data were collected using a Pilatus 300K detector (pixel size of 0.172 x 0.172 mm^2) positioned approximately 240 cm downstream of the sample. The SAXS flight path was helium-filled, and a beamstop photodiode was used to monitor transmitted intensity. SAXS data were collected using a 3 s exposure time. Acquired 2D SAXS data was reduced using the Nika and Irena macros[3,4] in Igor Pro 7 (WaveMetrics, Inc.). 1D data was generated from azimuthal integration of the 2D data using silver behenate as the calibration standard. Following this data reduction, intensities were normalized by the diode count, and from this was subtracted the diode count-normalized background intensity.

Polymer morphology was determined from the ratios of scattering peaks relative to the principal scattering peak.

Conversion and Molecular Weight Data for Synthesis of PMOS-PIBVE-PMOS

Table S1: Data collected during the synthesis of PMOS-PIBVE-PMOS.

Entry	Reaction time (h)	IBVE conv. (%)	MOS conv. (%)	total conv. (%)	M_n^{theo} (kg/mol)	M_n^{RI} (kg/mol)	Đ[d]	M_n^{LS} (kg/mol)	M_n ABA[e] (kg/mol)
0	0	0	0	0	0	0	-	0	-
1[a]	0.17	9	0	9	5.8	-	-	-	-
2[a]	0.55	9	0	9	5.8	1.4	1.4	-	-
3	0.7	23	0	23	14.8	10.2	1.53	21.1	-
4	0.93	52	0	52	33.5	24.8	1.36	32.6	-
5	1.07	62	0	62	40.4	32.2	1.33	41.1	-
6	1.5	92	0	92	59.2	42.8	1.28	58.6	-
7[b, c]	2	100	0	100	64.6	45.7	1.33	59.2	-
8	3	96	0	96	66.1	46.9	1.33	63.8	63.8
9	4.63	100	6	106	66.5	48.8	1.31	-	65.7
10	6.05	100	11	111	68	50.9	1.27	-	67.8
11	8.05	100	20	120	70.8	53.1	1.23	-	70
12	20.7	100	64	164	84.4	63.6	1.19	-	80.5
13	25.83	100	77	177	88.4	63.9	1.18	-	80.8
14	27.77	100	80	180	89.3	63.1	1.19	-	80
15	32.3	100	83	183	90.2	66.5	1.19	-	83.4
16	46.07	100	89	189	92.1	66.4	1.18	-	83.3
17	64.9	100	91	191	92.7	68	1.18	-	84.9

[a] No light scattering data available, not included in plot (Figure 3). [b] ^{1}H NMR showed no IBVE, however, due to IBVE being present in entry 8 ^{1}H NMR, it was assumed the IBVE must have evaporated from this sample and it was not included in the plot (Figure 3). [c] MOS was added after 2 hours, just after entry 7. [d] *Đ* was determined from the SEC trace. [e] M_n was calculated as shown in Equation S5.

Equation S5:

$$M_{\mathrm{n}}\ \mathrm{ABA} = M_{\mathrm{n}}^{\mathrm{RI}} Entry\ n - M_{\mathrm{n}}^{\mathrm{RI}}\ Entry\ 8 + M_{\mathrm{n}}^{\mathrm{LS}}\ Entry\ 8$$

The PMOS homopolymer peak in the GPC prevented proper determination of the refractive index increment (dn/dc) and thus the M_{n}s reported for the ABA copolymers are calculated from refractive index traces in SEC to polystyrene standards as illustrated in Figure S2.

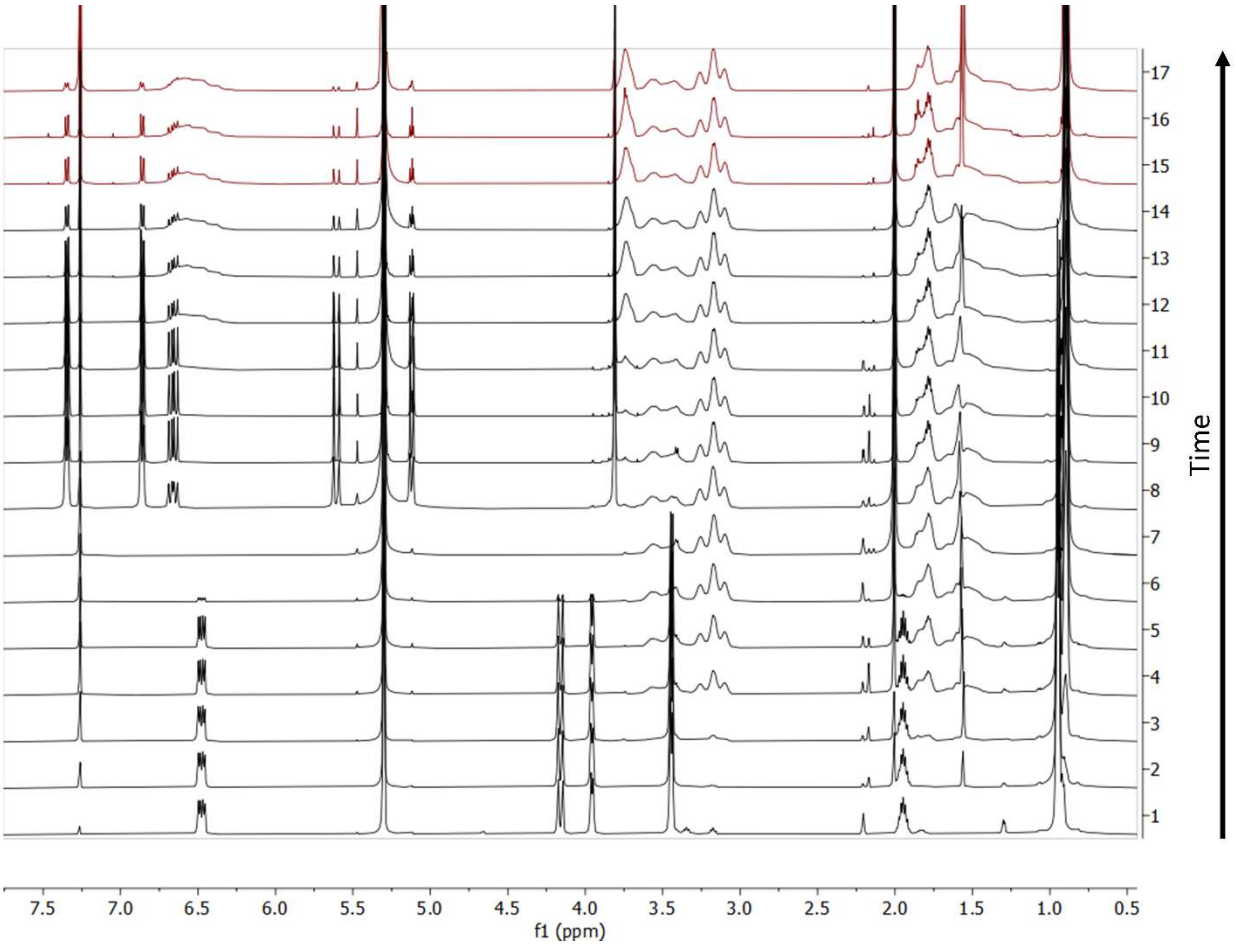

Figure S1: Quantitative ^{1}H NMR in $CDCl_3$ of aliquots from PMOS-PIBVE-PMOS reaction over time, reported in Table S1.

Material Characterization

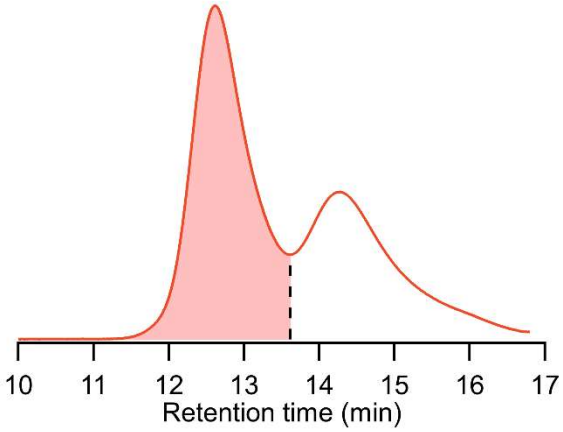

Figure S2: SEC trace of PMOS-PIBVE-PMOS illustrating how the peak for ABA copolymers were selected for M_n and $Đ$ calculations against polystyrene standards.

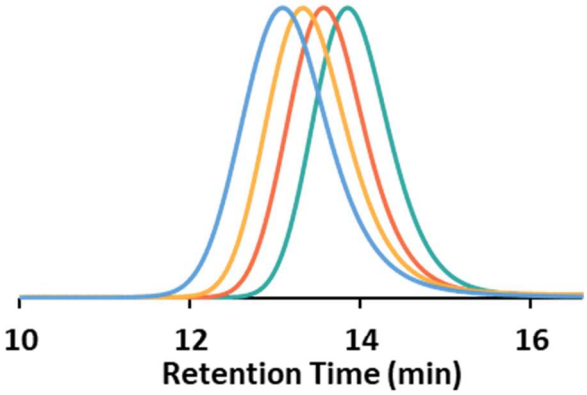

Entry	[IBVE]/ [CTA]	NMR Conv.	M_n (theo) (kg/mol)	M_n (exp) (kg/mol)	$Đ$
1	200	100%	20	23	1.32
2	300	100%	30	33	1.28
3	400	100%	40	41	1.25
4	500	100%	50	53	1.34

Figure S3: Polymerizations of telechelic PIBVE from a difunctional CTA.

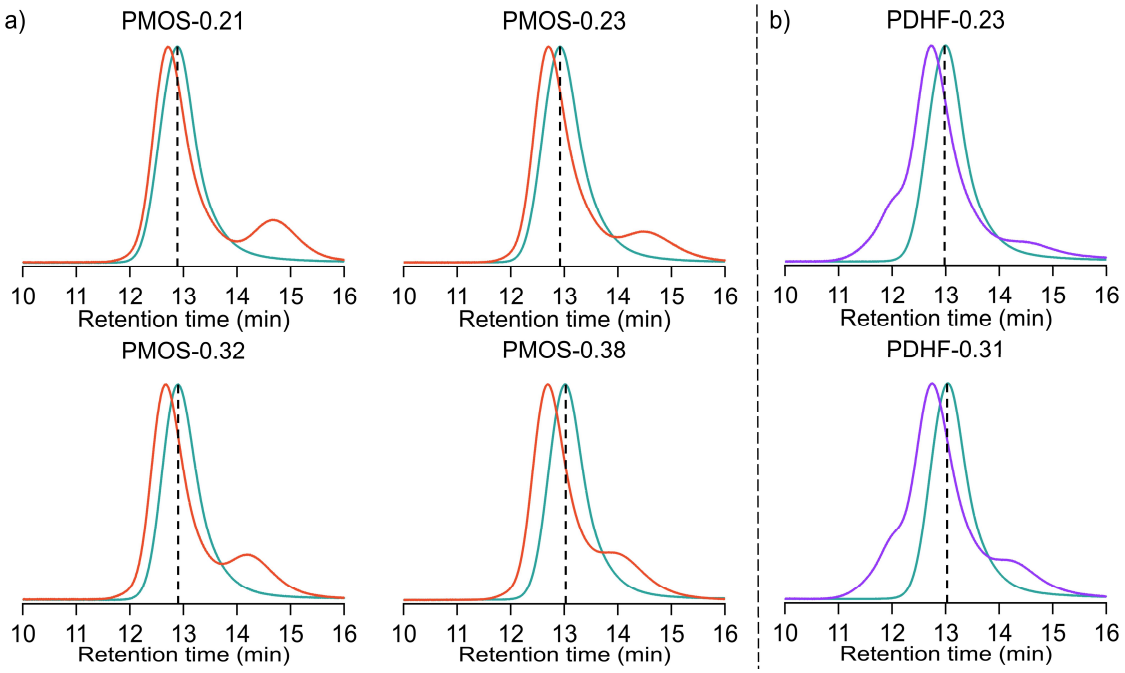

Figure S4: SEC traces of a) PMOS-PIBVE-PMOS (red) and b) PDHF-PIBVE-PDHF (blue) copolymers showing the chain extension from telechelic PIBVE (teal).

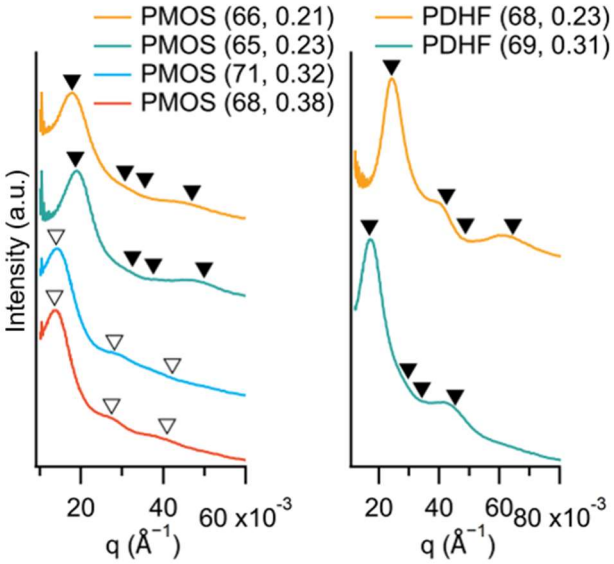

Figure S5: SAXS data obtained for each polymer sample. Braggs reflections for hexagonally packed cylinders (filled triangles) and lamellar (open triangles) morphologies are indicated, relative the first indicated peak, defined as q*.

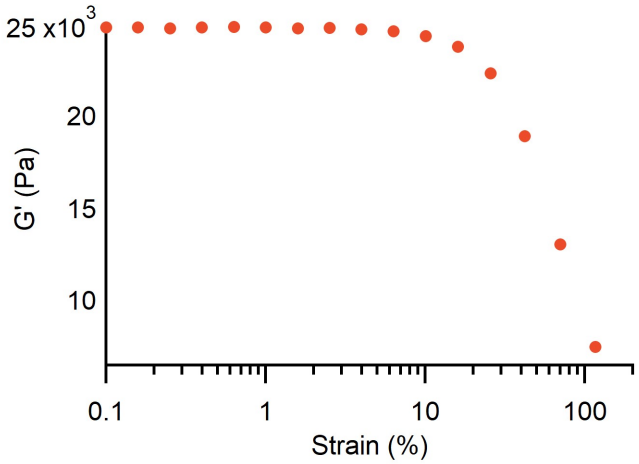

Figure S6.1: Strain sweep of PMOS-PIBVE-PMOS, from 0.1 to 100% strain, 1 Hz, 150 °C.

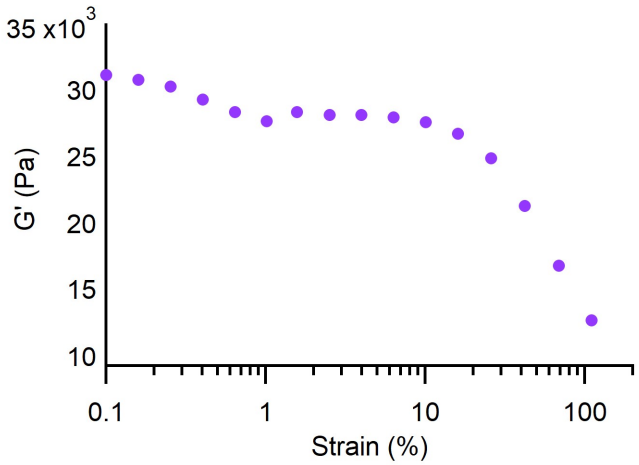

Figure S6.2: Strain sweep of PDHF-PIBVE-PDHF, from 0.1 to 100% strain, 1 Hz, 170 °C.

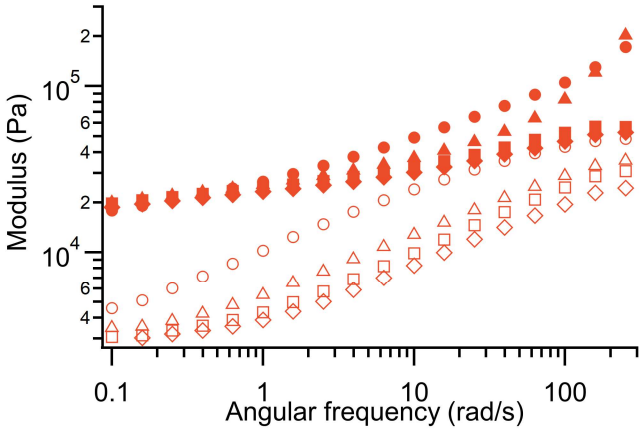

Figure S6.3: Frequency sweep of PMOS-0.21 (circles), PMOS-0.23 (triangles), PMOS-0.32 (squares), and PMOS-0.38 (diamonds) at 170 ºC. Filled markers correspond to G' and open markers correspond to G".

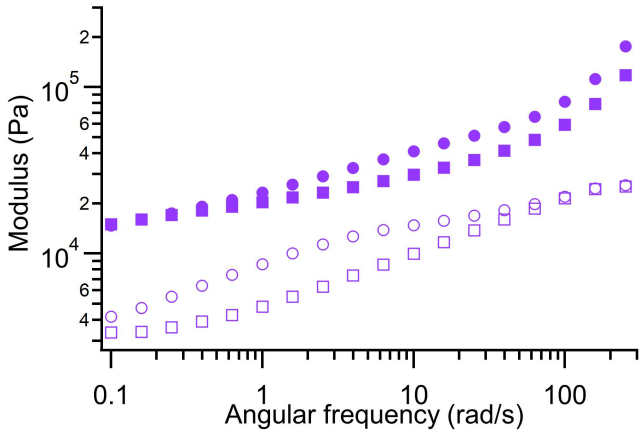

Figure S6.4: Frequency sweep of PDHF-0.23 (circles) and PDHF-0.31 (squares) at 170 ºC. Filled markers correspond to G' and open markers correspond to G".

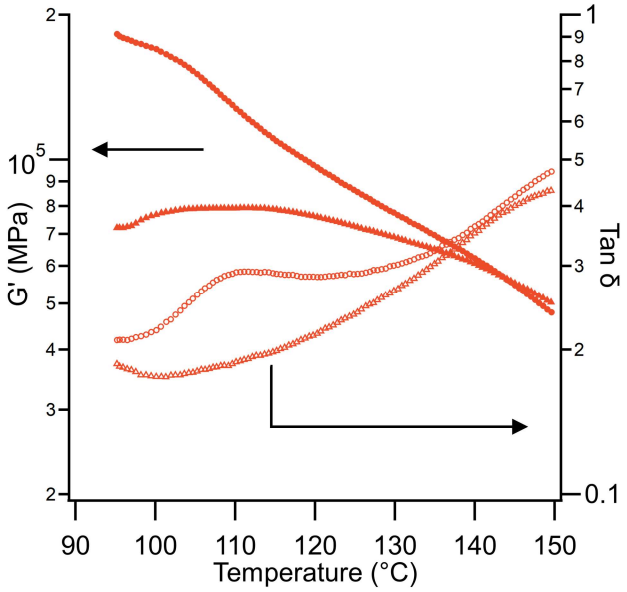

Figure S6.5: Temperature sweep of PMOS-0.38 (circles) and PMOS-0.32 (squares). Filled markers correspond to G' and open markers correspond to tan δ. The tan δ peak at 111 °C corresponds to the T_g of PMOS.

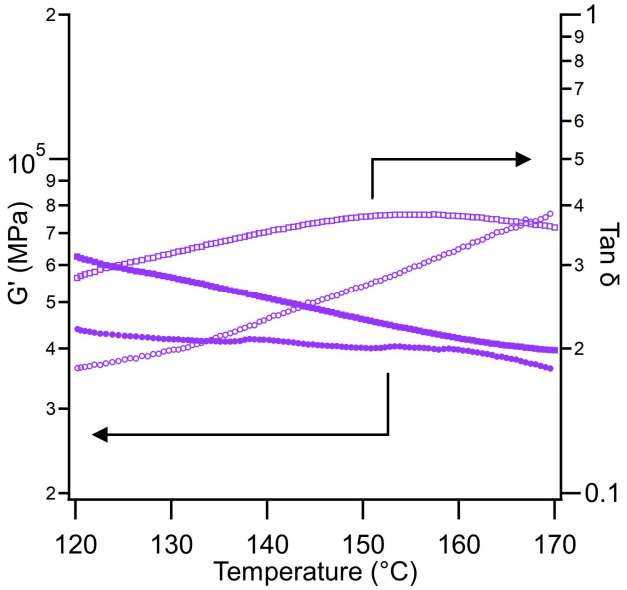

Figure S6.6: Temperature sweep of PDHF-0.31 (circles) and PDHF-0.23 (squares). Filled markers correspond to G' and open markers correspond to tan δ. No tan δ peak is observed due to the low volume fraction of PDHF.

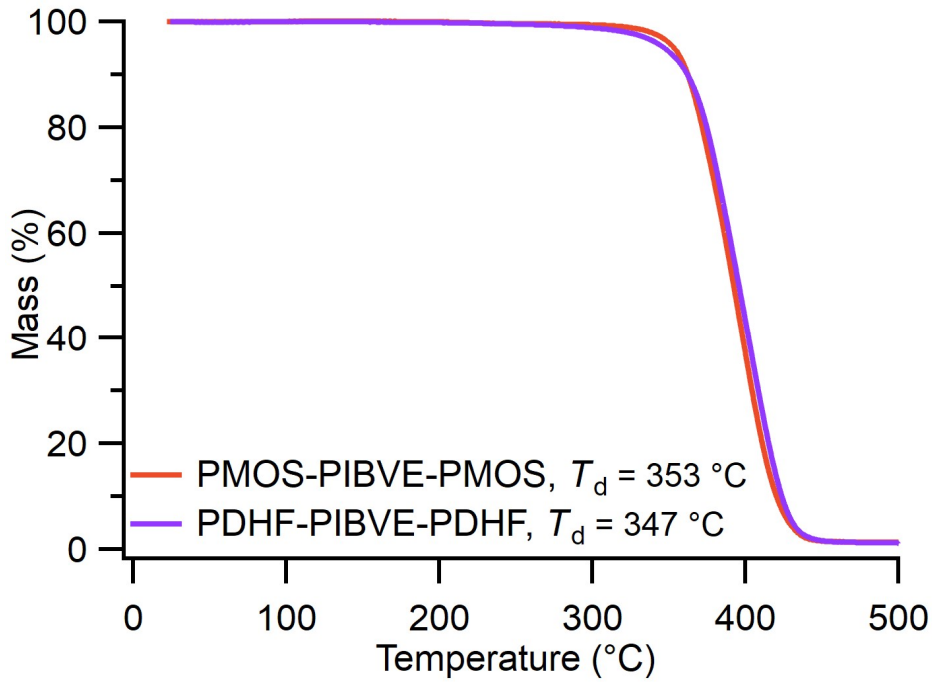

Figure S7: Thermal gravimetric analysis of mass vs. temperature (increased 10 °C/min) traces of each ABA copolymer. Degradation temperatures reported at 5% mass loss.

NMR Spectra:

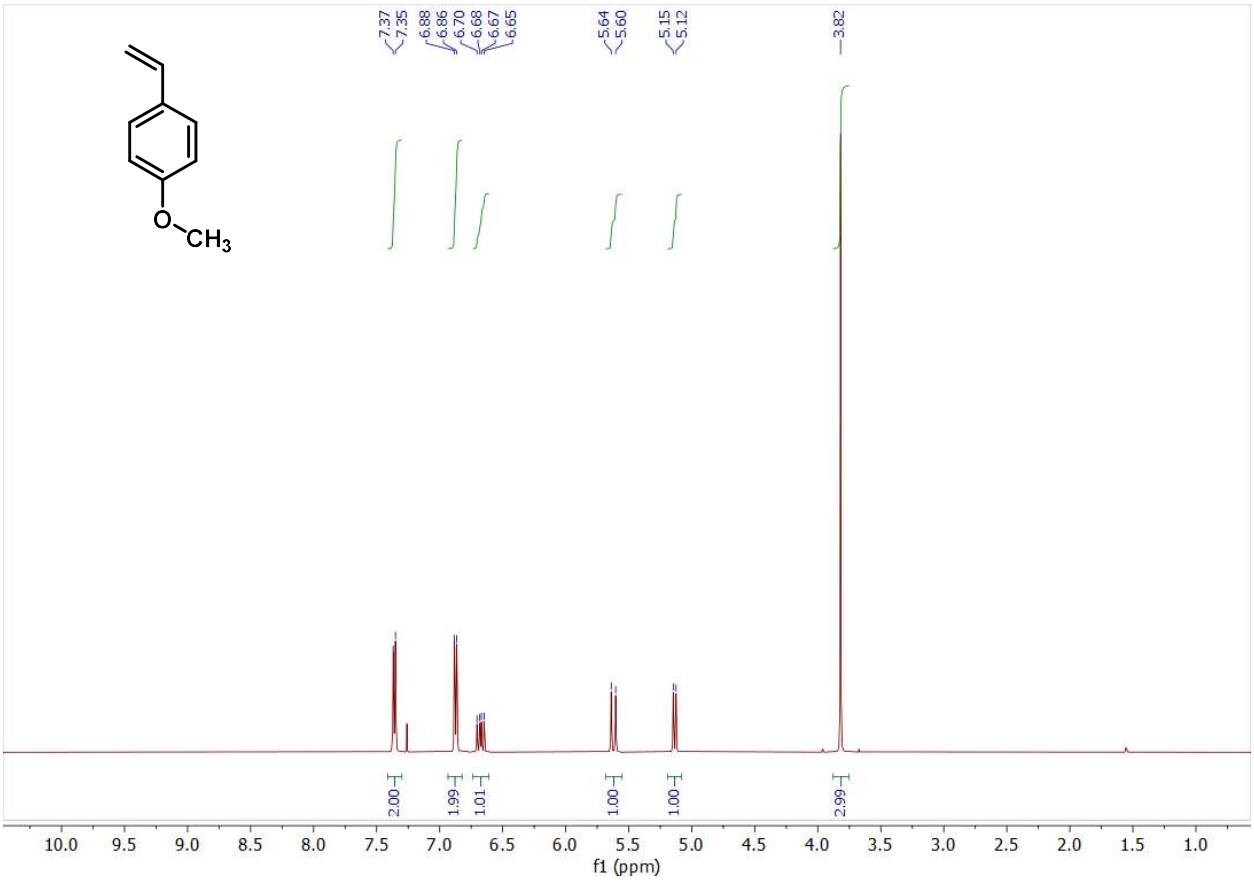

Figure S8.1: Quantitative ^{1}H NMR of *p*-methoxystyrene in $CDCl_3$

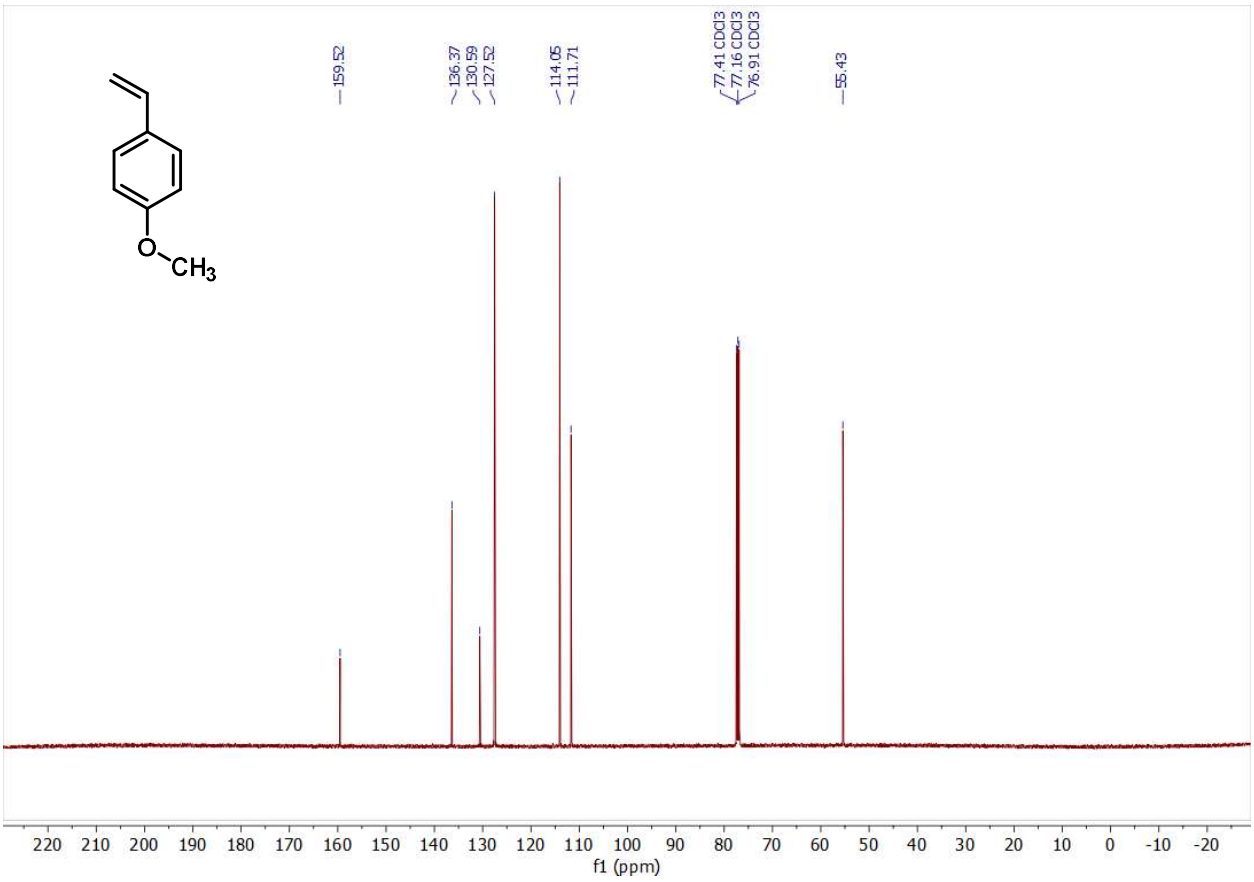

Figure S8.2: ^{13}C NMR of *p*-methoxystyrene in $CDCl_3$

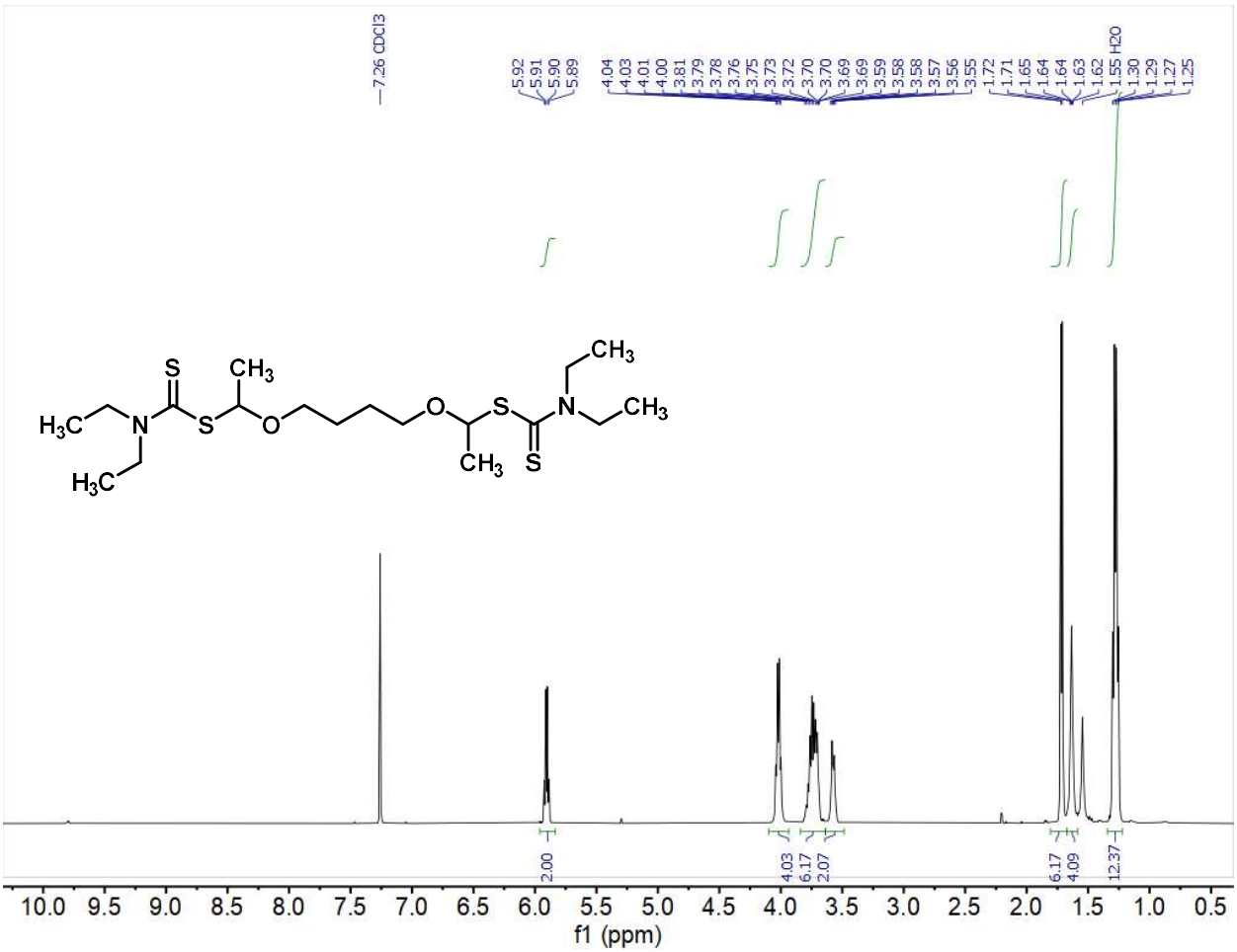

Figure S9.1: Quantitative ^{1}H NMR of difunctional CTA in $CDCl_3$

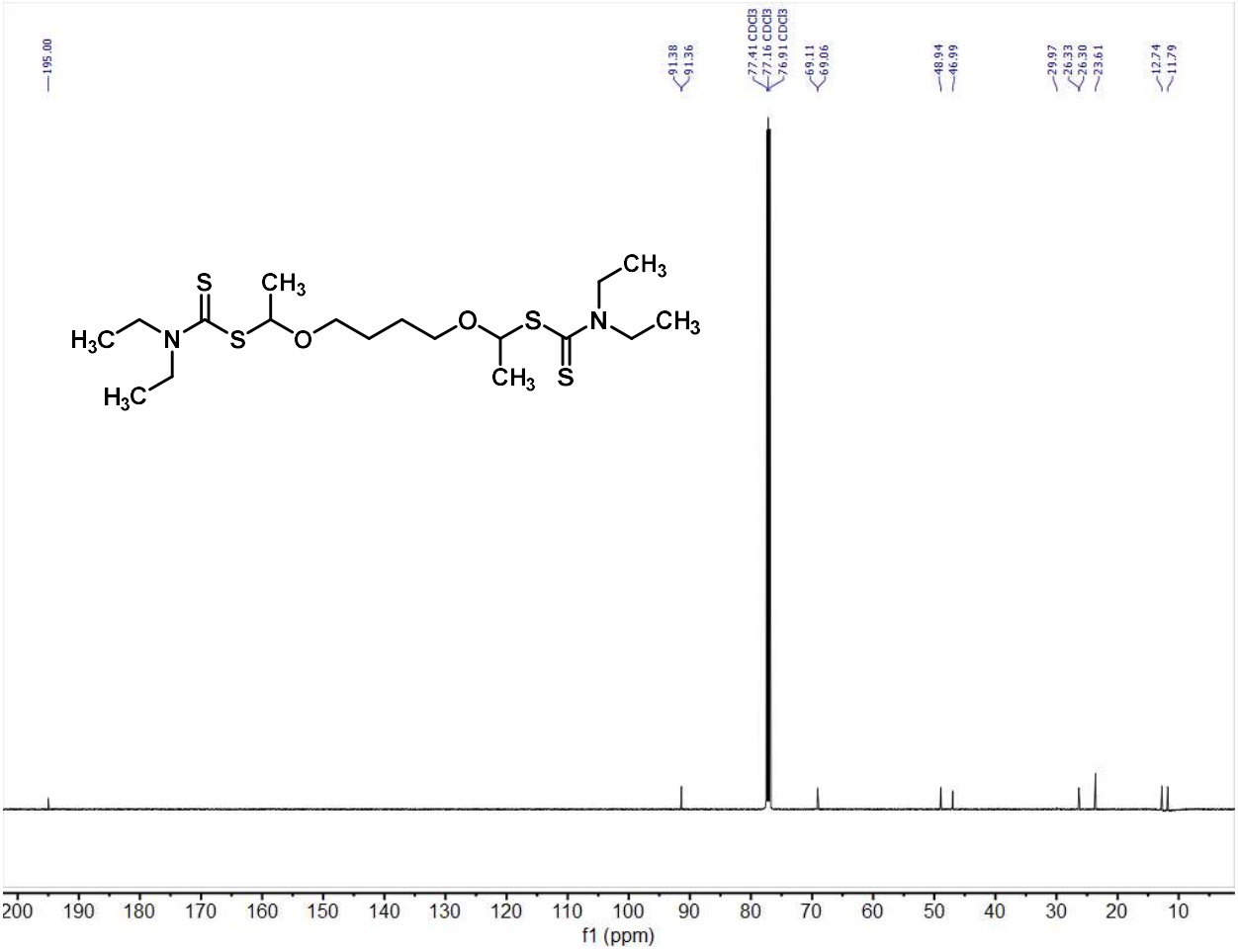

Figure S9.2: ^{13}C NMR of Difunctional CTA in $CDCl_3$

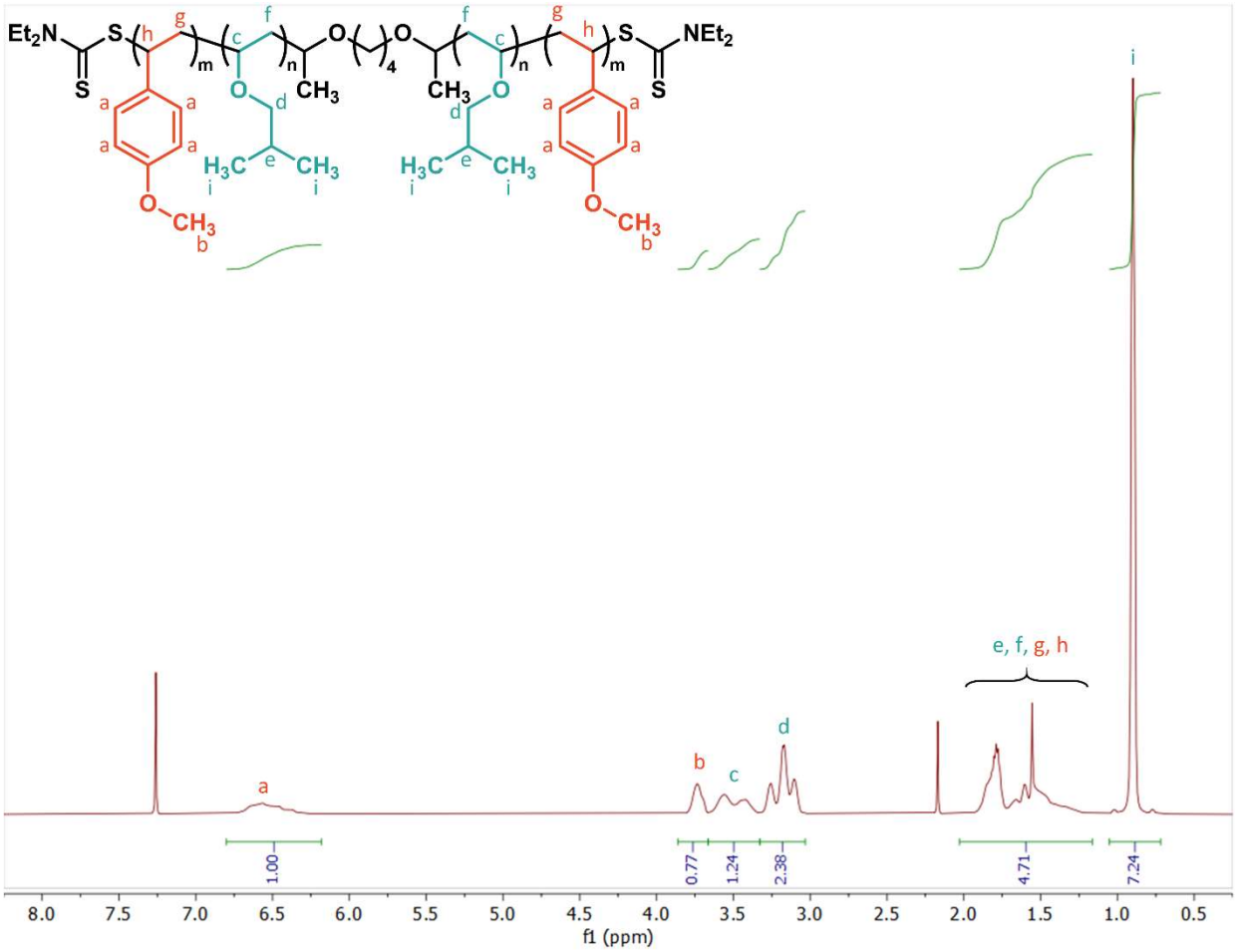

Figure S10.1: Quantitative ^{1}H NMR of PMOS-0.21 in $CDCl_3$

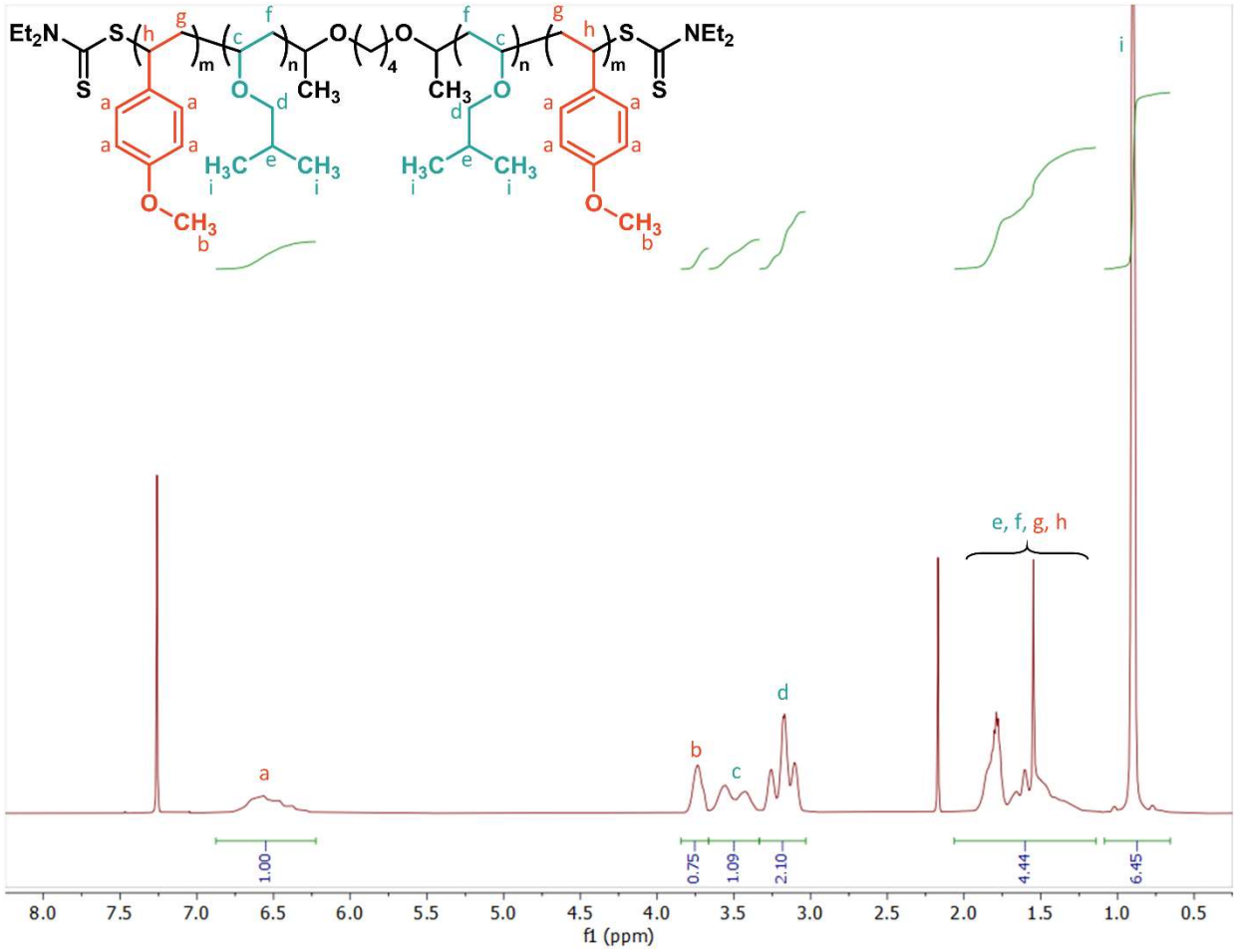

Figure S10.2: Quantitative ^{1}H NMR of PMOS-0.23 in $CDCl_3$

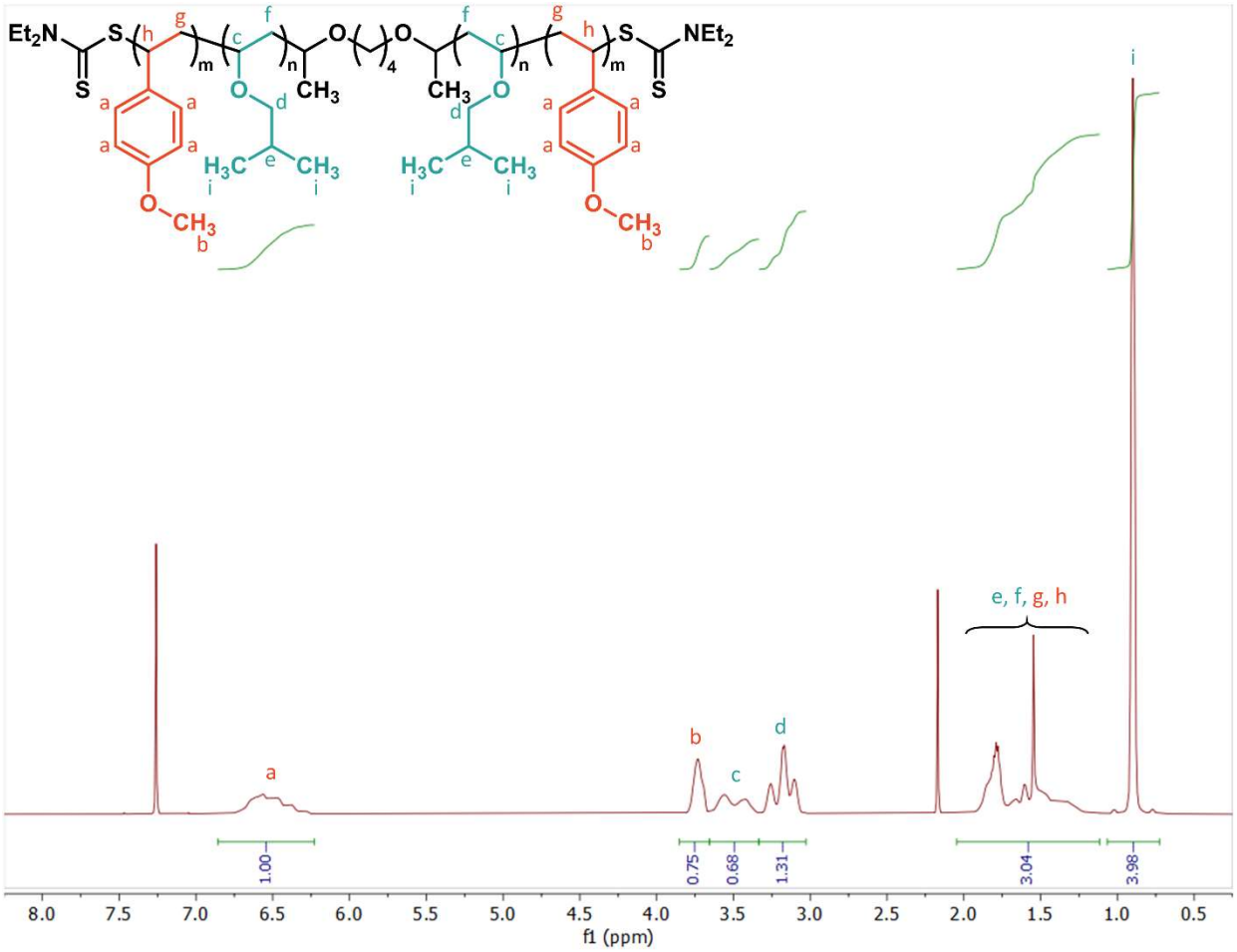

Figure S10.3: Quantitative ^{1}H NMR of PMOS-0.32 in $CDCl_3$

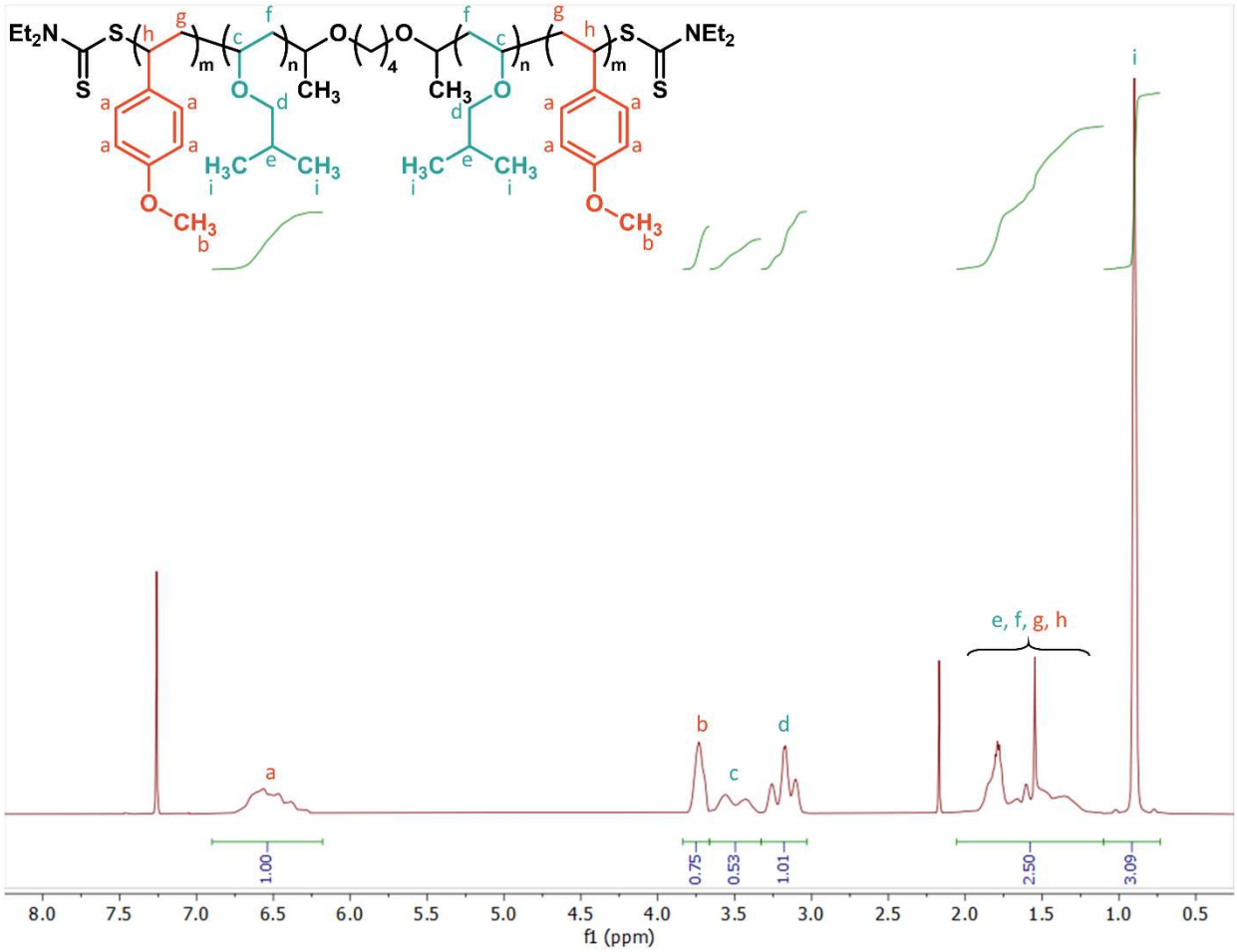

Figure S10.4: Quantitative ^{1}H NMR of PMOS-0.38 in $CDCl_3$

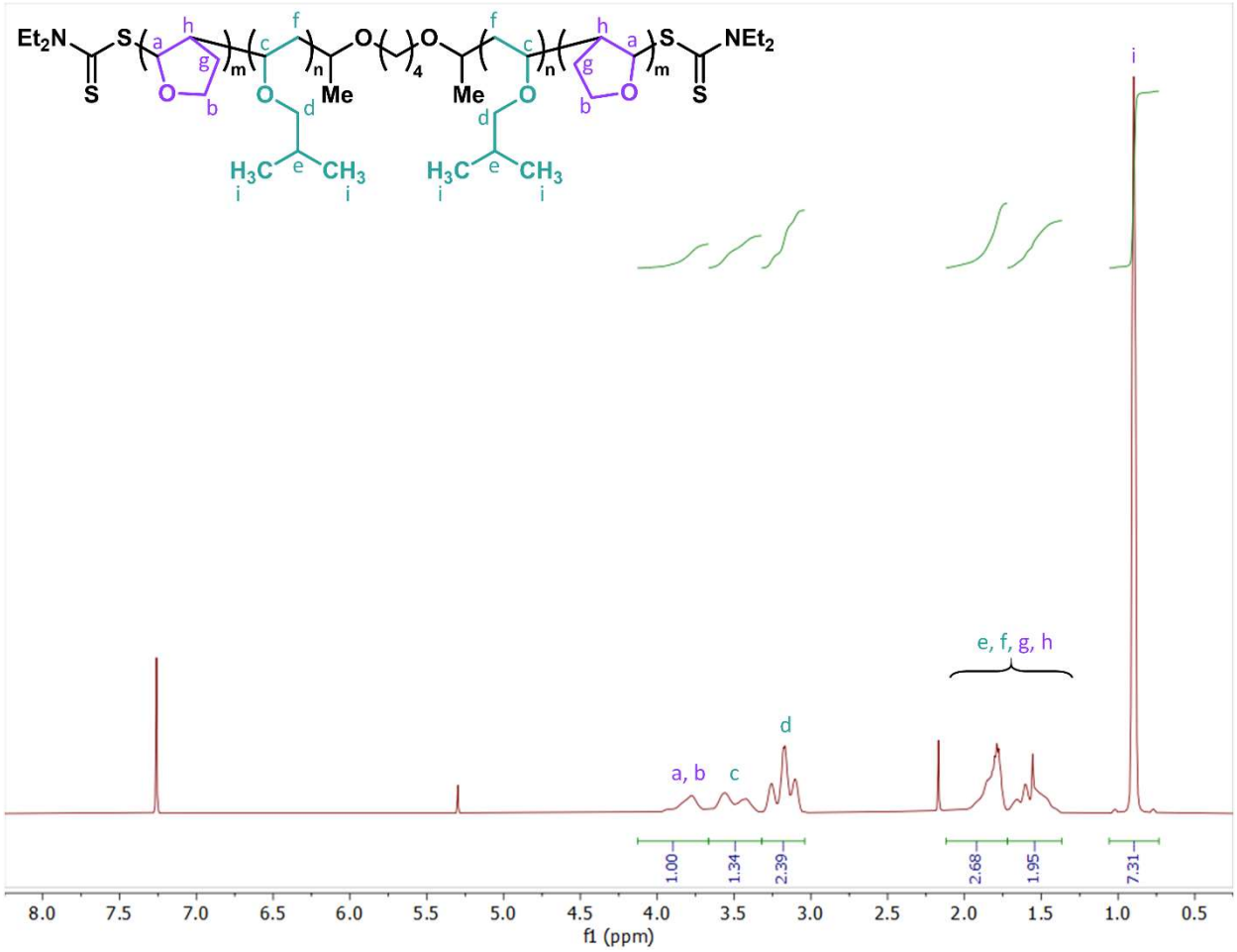

Figure S10.5: Quantitative ^{1}H NMR of PDHF-0.23 in $CDCl_3$

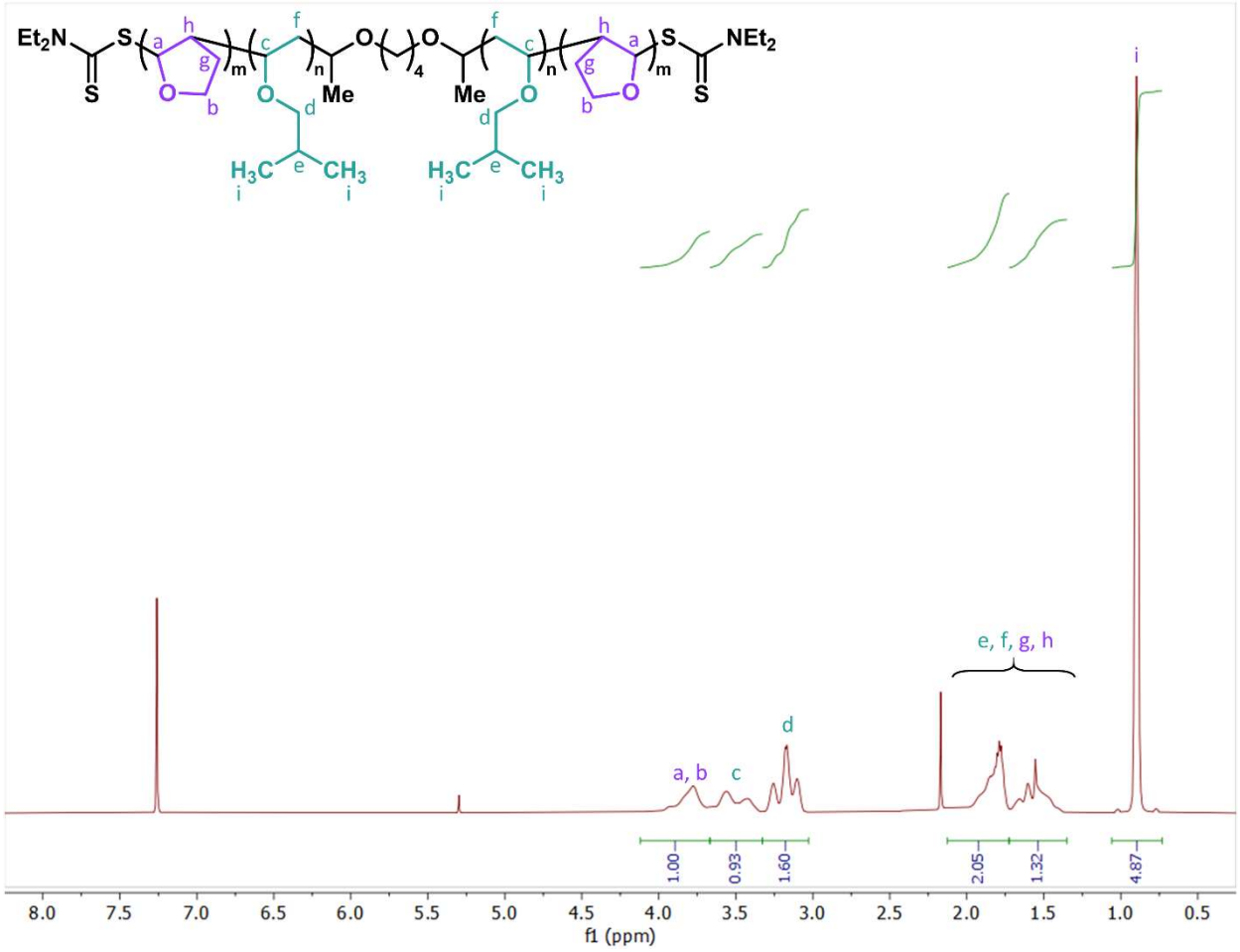

Figure S10.6: Quantitative ^{1}H NMR of PDHF-0.31 in $CDCl_3$

Green Metrics:

We evaluated the monomer and polymer syntheses disclosed herein using several widely accepted green metrics. Reported in Table S2 are the calculated isolated yields, atom economies (AEs) and process mass intensities (PMI). AE evaluates the percent molecular weight of the desired product compared to the molecular weight of all reactants.[5] For an account of all resources required in a process, the PMI is calculated as the mass of product divided by the mass of all reagents, solvents, and catalysts used in the reaction, workup, and purification.[6,7]

The synthesis of MOS has a high isolated yield (77%) over two steps on 25g scale. This reaction has a low AE due to the first step, decarboxylation of *p*-coumaric acid, resulting in mass loss from the original reactant. The methylation with methyl iodide is also inefficient due to the loss of iodide. The PMI is equally high for this process at 33 kg kg^{-1}. While this synthesis is not well-optimized in relation to green metrics, it does demonstrate the ability to source MOS, a common monomer in cationic RAFT polymerizations, from biomass.

The polymerizations of PMOS-PIBVE-PMOS and PDHF-PIBVE-PDHF are both ideal in AE, at 100%. This combined with high isolated yields (>70%), validates the efficiency of our cationic polymerization in producing ABA copolymers. While the PMI for each polymerization is high, this comes from the amount of methanol used to crash out the polymer for purification. However, the only byproducts left over are unreacted monomer, solvent, and ferrocene. The unreacted monomer and solvent can be removed under vacuum and, depending on the application of the polymer, the removal of ferrocene (0.07 wt%) would not be required, reducing the PMI by over 200%.

Table S2: Atom Economy and Process Mass Intensity

Product	Isolated Yield (%)	AE[a] (%)	PMI[b] (kg kg^{-1})	PMI without precipitation in MeOH (kg kg^{-1})
MOS	77	44	33	–
PMOS-PIBVE-PMOS	75	100	910	3.8
PDHF-PIBVE-PDHF	71	100	1146	4.3

[a] Defined as the percent molecular weight of the product compared to the molecular weight of all reactants. [b] Defined as the mass of isolated product to mass of all materials used.

Equation S6:

$$AE\ (\%) = \frac{molecular\ weight\ of\ product}{molecular\ weight\ of\ reactants} \times 100$$

Equation 7 was used to calculate the process mass index (PMI), which takes into account the mass of all reactants and solvents used in the reaction, work up, and purification.

Equation S7:

$$PMI = \frac{total\ mass\ of\ materials\ used\ in\ process\ (kg)}{mass\ of\ isolated\ product\ (kg)}$$

Peak Deconvolution of SEC Traces

In addition to the previously described method for estimating the molecular weight of these triblock copolymers, we also utilized peak deconvolution. Peak deconvolution is often performed to estimate molecular weights and mass fractions in multimodal polymer molecular weight distributions. To do so, we converted differential distributions to plots of mass fraction versus molecular weight. It is important to note that these molecular weights are calculated based on polystyrene standards and are not absolute. Furthermore, without knowing the higher moments of the polymer molecular weight distributions, peak deconvolution does not afford highly accurate values. For these reasons, the data provided below is offered only as a comparison to the aforementioned method for calculating molecular weights. The Multipeak Fitting Package in Igor Pro 7 was utilized for peak deconvolution (Figure S11). PMOS triblock copolymers were assumed to have bimodal distributions whereas PDHF triblock copolymers were assumed to have trimodal distributions. All peaks were fit to a Gaussian function except for the highest molecular weight peaks in PDHF polymers (peak 3), which were fit to a Lorentzian function. From these peak fits were calculated M_n (equation S8) and the mass percent of each peak (equation S9). These values are displayed in Table S3.

Equation S8:

$$M_n = \frac{\sum M_i * N_i}{\sum N_i}$$

Equation S9:

$$mass\ \% = 100 \times \frac{\sum N_{i,peak\ 1}}{\sum (N_{i,peak\ 1} + N_{i,peak\ 2})}$$

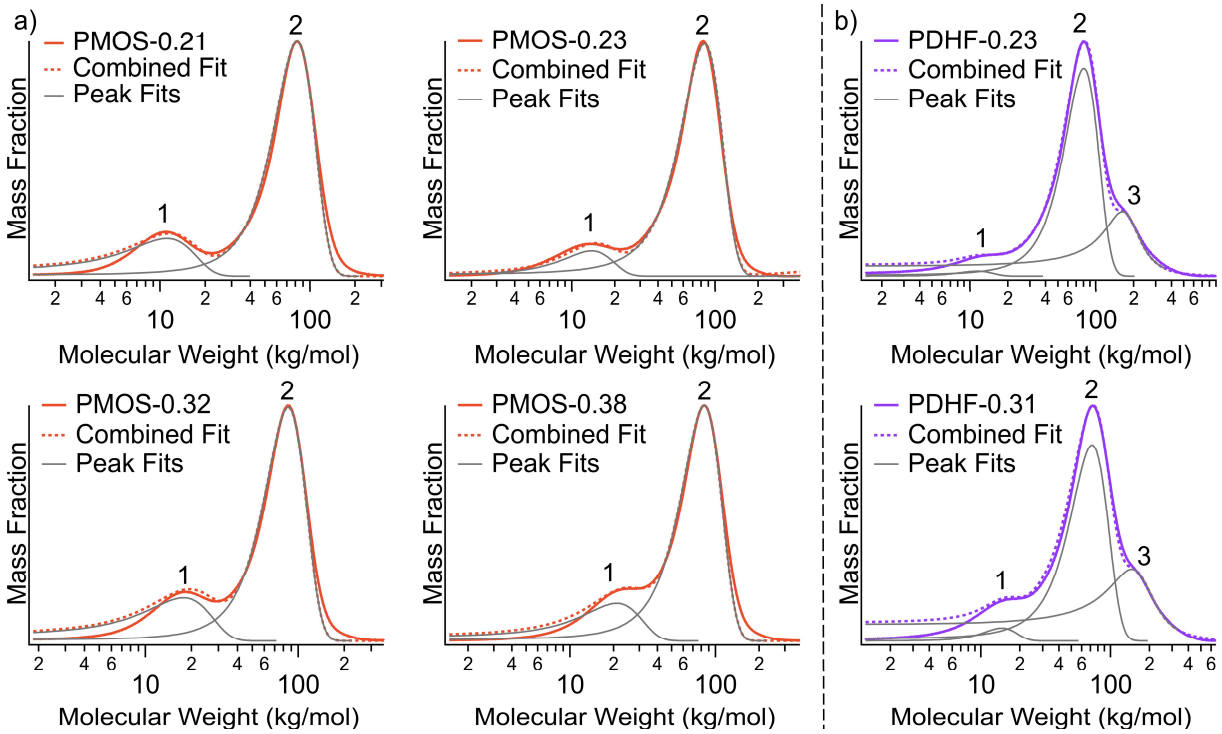

Figure S11: Peak deconvolution of a) PMOS-PIBVE-PMOS and b) PDHF-PIBVE-PDHF SEC traces calculated using the Multipeak Fitting Package in Igor Pro 7.

Table S3: ABA copolymer composition calculated from peak fitting data.

Sample	Peak 1 M_n (kg/mol)	Peak 2 M_n (kg/mol)	Peak 3 M_n (kg/mol)	Mass % (Peak 1:Peak 2:Peak 3)
PMOS-0.21	11.6	82.0	–	16:84
PMOS-0.23	13.9	84.3	–	2:98
PMOS-0.32	18.4	85.9	–	16:84
PMOS-0.38	21.4	83.8	–	15:85
PDHF-0.23	11.5	80.3	167	1:67:32
PDHF-0.31	14.5	72.1	153	2:59:38

References

1 A. J. Perkowski, W. You and D. A. Nicewicz, *J. Am. Chem. Soc.*, 2015, **137**, 7580–7583.

2 S. Stoupin, J. P. C. Ruff, T. Krawczyk and K. D. Finkelstein, *Acta Crystallogr. Sect. A*, 2018, **74**, 567–577.

3 J. Ilavsky, *J. Appl. Crystallogr.*, 2012, **45**, 324–328.

4 J. Ilavsky and P. R. Jemiana, *J. Appl. Crystallogr.*, 2009, **42**, 347—353.

5 M. Tobiszewski, M. Marć, A. Gałuszka and J. Namieśnik, *Molecules*, 2015, **20**, 10928–10946.

6 C. Jimenez-Gonzalez, C. S. Ponder, Q. B. Broxterman and J. B. Manley, *Org. Process Res. Dev.*, 2011, **15**, 912–917.

7 C. Jiménez-González, D. J. C. Constable and C. S. Ponder, *Chem. Soc. Rev.*, 2012, **41**, 1485–1498.